

Surface Wave Analysis for Vs30 Estimation Using Multichannel Analysis of Surface Waves (MASW)

Bhavik Patel¹

¹Department of CSE, IIT Gandhinagar
22110047

Hitesh Kumar²

²Department of CSE, IIT Gandhinagar
22110098

Sahil Mundlod³

³Department of EE, IIT Gandhinagar
22110161

Shaury Patel⁴

⁴Department of ME, IIT Gandhinagar
22110241

Abstract

This study presents a comprehensive implementation of Multi-channel Analysis of Surface Waves (MASW) for near-surface shear-wave velocity (V_s) profiling and site characterization. The methodology encompasses the complete MASW workflow, from raw seismic data processing to final site classification based on $Vs30$ values.

The analysis begins with seismic data preprocessing, including bandpass filtering (5-50 Hz) and trace normalization, followed by dispersion curve extraction using phase-shift methods to identify fundamental-mode Rayleigh wave velocities across multiple frequencies (5-50 Hz). Three inversion schemes were employed and compared: damped least-squares, Monte Carlo global search, and a hybrid approach combining both methods. The forward modeling uses the disba library for rigorous modal summation of fundamental-mode Rayleigh wave velocities in layered media.

Results from the hybrid inversion yield a six-layer velocity model extending beyond 30 meters depth, with $Vs30 = 287.6$ m/s. Uncertainty quantification through ensemble modeling of 100 acceptable Monte Carlo models demonstrates $Vs30 = 287.5 \pm 30.6$ m/s (95% CI: 227.6-347.5 m/s). The site is classified as NEHRP Site Class D (Stiff Soil) with site amplification coefficients $F_a = 1.60$ and $F_v = 2.40$.

This work demonstrates the effectiveness of MASW as a non-invasive geophysical technique for shallow subsurface characterization, with direct applications in seismic hazard assessment, geotechnical site investigation, and earthquake engineering.

Github Link: <https://github.com/bp0609/Multichannel-Analysis-of-Surface-Waves>

Keywords: MASW, surface waves, $Vs30$, dispersion analysis, phase shift method, inversion, Monte Carlo uncertainty, site classification, NEHRP, stiff soil.

1 Introduction

The accurate determination of subsurface shear-wave velocity (V_s) profiles is critical for seismic site characterization and earthquake engineering applications. The time-averaged shear-wave velocity to 30 meters depth ($Vs30$) serves as a primary parameter for seismic site classification in building codes worldwide, including the NEHRP (National Earthquake Hazards Reduction Program) provisions and ASCE 7-22 standards [1, 2].

Multichannel Analysis of Surface Waves (MASW) has emerged as a cost-effective and non-invasive geophysical method for determining near-surface V_s profiles [3, 4]. The method exploits the dispersive nature of surface waves (primarily Rayleigh waves) propagating through vertically heterogeneous media [5, 6]. Different frequency components of surface waves penetrate to different depths, with lower frequencies sampling deeper materials. By analyzing the frequency-dependent phase velocity (dispersion curve), the subsurface V_s structure can be inferred through inversion.

This study aims to demonstrate a complete MASW workflow from data acquisition through final site classification, with emphasis on:

- Phase shift dispersion extraction method [7]
- Comparison of three inversion algorithms (least-squares, Monte Carlo, hybrid)
- Rigorous uncertainty quantification using ensemble modeling [8]
- NEHRP and Eurocode 8 site classification [2, 9]
- Engineering interpretation and design implications

2 Theoretical Background

2.1 Surface Wave Propagation

Surface waves propagate along the Earth's surface with particle motion confined primarily to the near surface. Rayleigh

waves, the dominant surface wave type in MASW surveys, exhibit elliptical retrograde particle motion in the vertical plane containing the propagation direction [5].

The dispersion relation for Rayleigh waves in a layered medium can be expressed as:

$$c(f) = c(V_s, V_p, \rho, h, f) \quad (1)$$

where $c(f)$ is the phase velocity at frequency f , V_s and V_p are shear and compressional wave velocities, ρ is density, and h represents layer thicknesses [5].

2.2 Dispersion Curve Analysis

The fundamental mode dispersion curve represents the relationship between phase velocity and frequency (or wavelength). The phase velocity at a given frequency is approximately related to the depth of investigation by:

$$z_{max} \approx \frac{\lambda}{2} = \frac{c(f)}{2f} \quad (2)$$

The phase shift method (also called f-c or τ -p transform) was employed for extracting dispersion curves from multi-channel seismic data [7, 10]. This approach analyzes phase coherence across receiver arrays in the frequency domain, evaluating the phase difference between adjacent receivers as a function of frequency to construct a dispersion image in the frequency-velocity domain.

2.3 Inversion Methods

The inverse problem seeks to find the Vs model that best explains the observed dispersion curve [4]. This study compares three approaches:

Damped Least-Squares: Iterative linearized inversion (Levenberg-Marquardt) minimizing:

$$\Phi = (d - g(m))^T C_d^{-1} (d - g(m)) + \alpha m^T C_m^{-1} m \quad (3)$$

where d is observed data, $g(m)$ is forward model prediction, and α is damping parameter.

Monte Carlo: Global search method exploring parameter space through random sampling with acceptance criteria based on RMS misfit threshold [8, 11].

Hybrid: Combines global Monte Carlo search for initial model exploration with local least-squares optimization for refinement.

2.4 Vs30 Calculation

Vs30 is calculated as the time-averaged shear-wave velocity to 30 meters depth [1]:

$$Vs30 = \frac{30}{\sum_{i=1}^n \frac{h_i}{V_{si}}} \quad (4)$$

where h_i and V_{si} are the thickness and shear-wave velocity of the i -th layer.

3 Data Acquisition and Survey Design

3.1 Data Source

The analysis utilized synthetic MASW data from Geophydog's Seismic Data Examples repository. The dataset consists of SAC (Seismic Analysis Code) binary format files representing an active source shot gather acquisition.

3.2 Acquisition Geometry

The MASW survey employed an active source configuration with the following parameters:

- Number of receivers: 60 geophones
- Receiver spacing: $dx = 1.0$ m
- Source offset: $x_1 = 10.0$ m
- Array length: 59.0 m
- Maximum offset: 69.0 m
- Sampling rate: 512.01 Hz
- Record length: 8 seconds
- Component: Vertical

Figure 1 and 2 illustrates the acquisition geometry in plan view and the receiver distribution along the survey line.

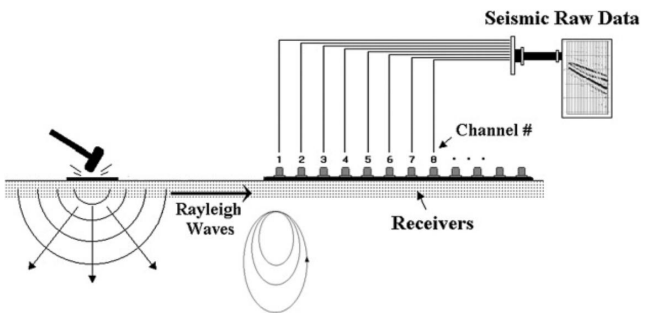


Figure 1: Experiment Setup

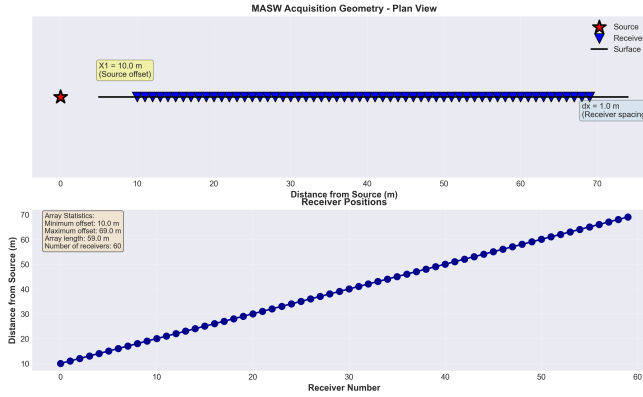


Figure 2: MASW acquisition geometry showing source position (star), receiver array (triangles), and array statistics. The linear receiver array extends from 10m to 69m from the source.

The source offset of 10 meters was chosen to ensure adequate surface wave generation while minimizing near-field effects [3, 12]. The 1-meter receiver spacing provides good spatial sampling for the target frequency range of 5-50 Hz.

Note: The SAC file distance headers contained a unit scaling issue (stored in km instead of m), requiring a correction factor of 1000 \times applied to all distance values during data loading.

3.3 Raw Seismic Data

The raw seismograms display characteristic surface wave arrivals with amplitude decay as a function of offset. Figure 3 shows the complete 60-trace shot gather.

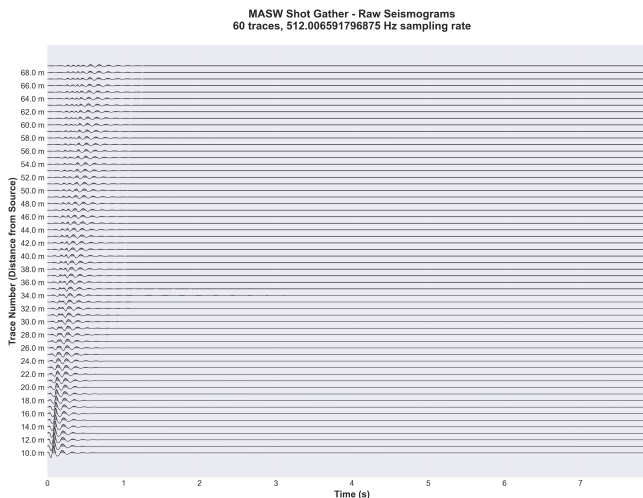


Figure 3: Raw MASW shot gather showing 60 seismic traces. Surface wave arrivals are clearly visible with coherent phase across the array. Note the amplitude decay with increasing distance from source.

3.4 Individual Trace Analysis

Detailed waveform analysis of individual traces reveals the multi-frequency nature of surface wave signals. Figure 4 displays representative traces at various offsets.

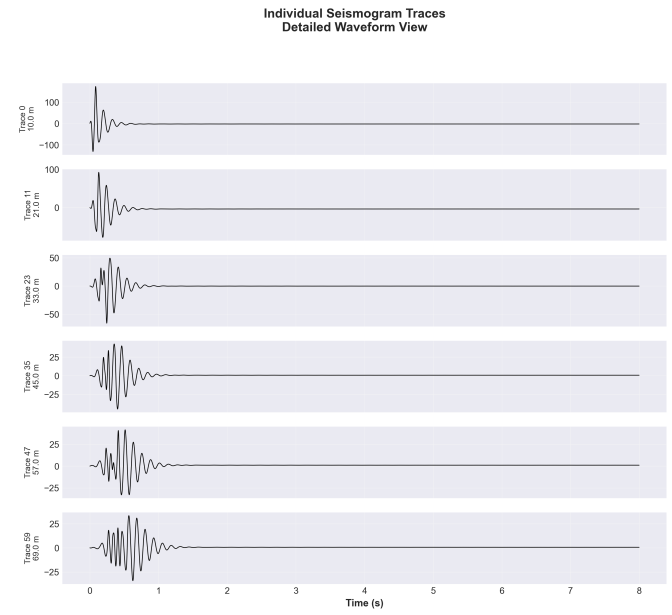


Figure 4: Individual seismogram traces at selected receiver positions showing detailed waveform characteristics. The complex waveforms result from superposition of multiple frequency components.

4 Data Processing and Analysis

4.1 Preprocessing

Signal preprocessing is essential for optimal dispersion curve extraction [10, 12]. The following processing workflow was implemented:

- **Bandpass filter:** 5-50 Hz, 4th-order Butterworth filter, zero-phase
- **Trace normalization:** Amplitude normalization applied to each trace independently
- **Quality control:** Removal of NaN/Inf values

The frequency band (5-50 Hz) was selected based on spectral analysis of the raw data to maximize surface wave energy while suppressing noise. Figure 5 compares original and processed data, demonstrating improved surface wave clarity.

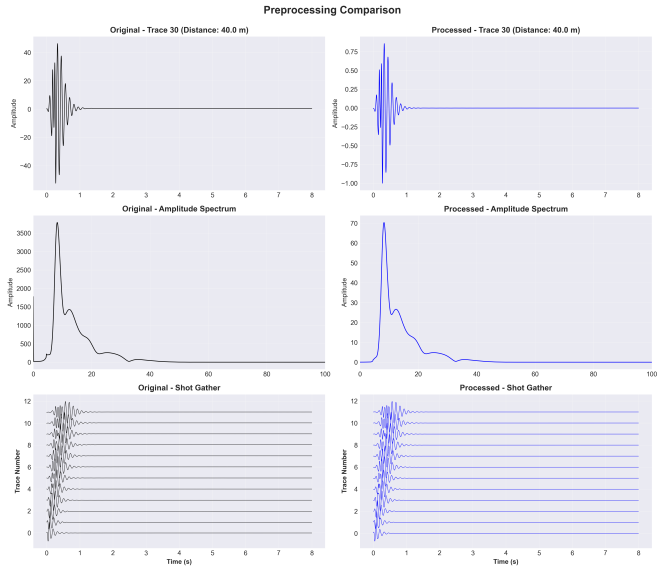


Figure 5: Comparison of original (left) and preprocessed (right) seismic data for a representative trace. Preprocessing enhances surface wave energy while suppressing noise and unwanted arrivals.

All 60 processed traces were saved as SAC files with processing parameters logged for reproducibility.

4.2 Frequency Content Analysis

Spectral analysis reveals the frequency characteristics of the recorded signals [10]. Figure 6 shows amplitude and power spectra at different offsets.

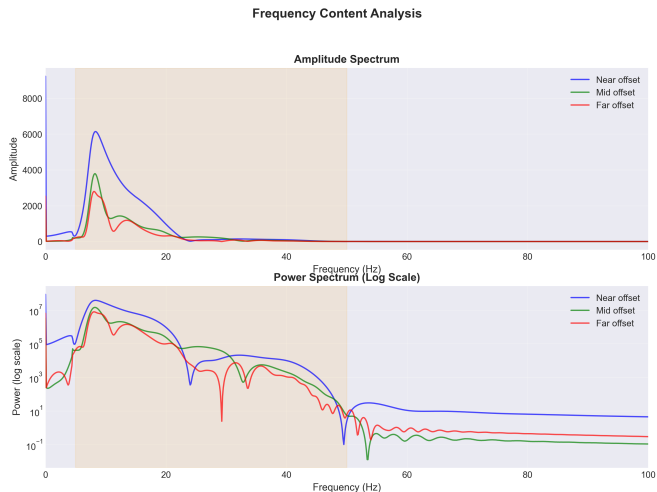


Figure 6: Frequency content analysis showing amplitude spectra at near, mid, and far offsets. The shaded region (5-50 Hz) indicates the bandpass filter limits used for dispersion analysis.

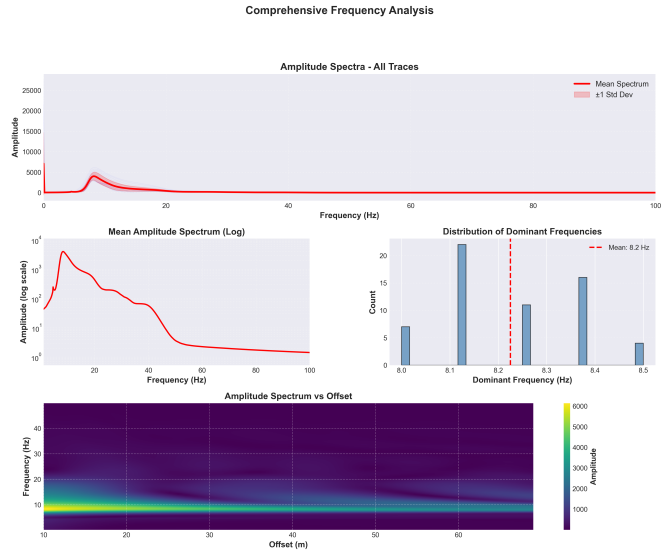


Figure 7: Comprehensive frequency analysis including amplitude spectra across all traces, mean spectrum (log scale), distribution of dominant frequencies, and amplitude spectrum versus offset. This analysis guided the selection of the 5-50 Hz processing band.

4.3 Dispersion Analysis

4.3.1 Phase Shift Method

The phase shift method was employed for dispersion curve extraction from the multichannel seismic data [7]. This approach analyzes the phase coherency of surface waves across the receiver array as a function of frequency and phase velocity, constructing a dispersion image in the frequency-velocity domain.

Analysis parameters:

- Frequency range: 5.0 - 50.0 Hz
- Number of frequency samples: 450
- Velocity range: 100.0 - 800.0 m/s
- Number of velocity samples: 500

The phase shift method applies cylindrical spreading correction to account for geometric attenuation of surface waves. For each trial phase velocity and frequency combination, the method calculates the expected phase shift between receivers and evaluates the coherence of energy across the array. High coherence indicates the presence of surface wave energy traveling at that particular velocity.

Figure 8 presents the resulting dispersion image. The fundamental mode Rayleigh wave is clearly identified as a high-energy trend, spanning the full frequency range with phase velocities between 174-665 m/s.

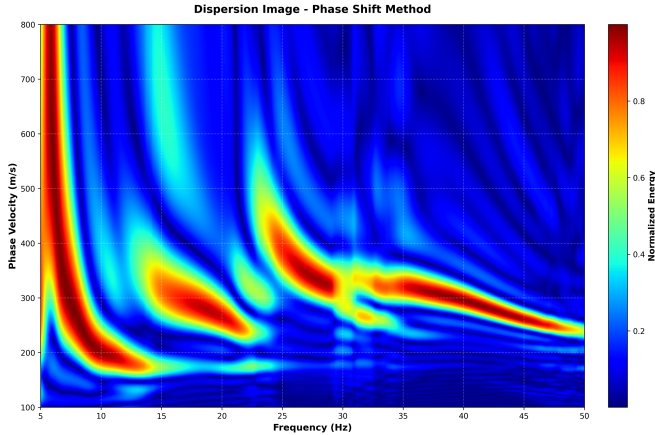


Figure 8: Dispersion image using phase shift method with cylindrical spreading correction. The fundamental mode is visible as the high-energy trend (warm colors). The picked dispersion curve is shown as overlaid points.

The phase shift method produced a clean dispersion image with minimal artifacts, making it well-suited for automatic picking algorithms [12]. The clear separation between fundamental mode energy and background noise provides confidence in the extracted dispersion curve.

4.3.2 Automatic Dispersion Curve Extraction

An automatic picking algorithm was applied to extract the fundamental mode dispersion curve from the phase shift dispersion image. The algorithm identifies the maximum energy along each frequency slice, effectively tracing the ridge of highest coherence in the frequency-velocity domain.

Figure 9 shows the dispersion image with the automatically picked fundamental mode curve overlaid as colored points. The picker successfully follows the fundamental mode trend across the entire frequency range without manual intervention.

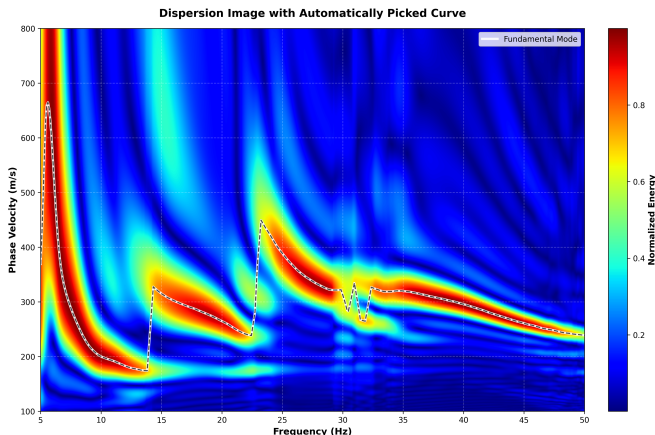


Figure 9: Dispersion image with automatically picked fundamental mode curve. The picking algorithm identifies maximum energy along the frequency axis, successfully tracing the fundamental mode across the full bandwidth.

4.3.3 Observed Dispersion Curve

The final extracted dispersion curve spans the frequency range of 5-50 Hz with phase velocities between 174.1-664.8 m/s. Figure 10 displays the observed dispersion curve with uncertainty estimates derived from the width of the energy peak at each frequency.

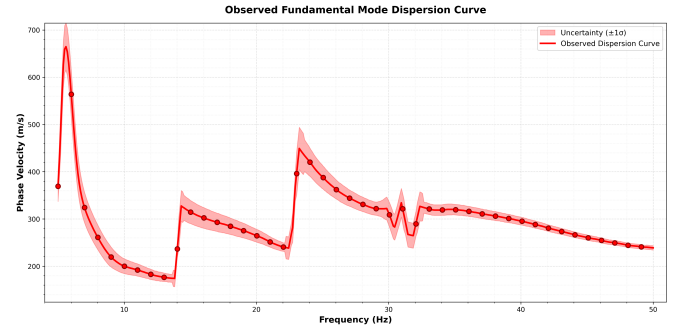


Figure 10: Observed fundamental mode dispersion curve with error bars representing picking uncertainty (mean = 16.5 m/s). The increasing velocity with decreasing frequency indicates velocity increase with depth. This improved figure features wider spacing and cleaner visualization.

Key characteristics:

- Velocity range: 174.1 - 664.8 m/s
- Wavelength range: 4.8 - 119.9 m
- Estimated maximum depth: ~ 120 m ($\lambda_{max}/2$)
- Mean picking uncertainty: 16.5 m/s

The dispersion curve exhibits a gradual velocity increase with decreasing frequency (increasing wavelength), indicating a velocity increase with depth. This is typical of consolidated sedimentary sequences. The maximum wavelength of 120 m suggests the dispersion curve samples depths well beyond the 30 m required for Vs30 calculation [12].

5 Inversion Results

5.1 Initial Earth Model

The initial model for inversion consisted of a simple layered structure based on preliminary analysis of the dispersion curve characteristics.

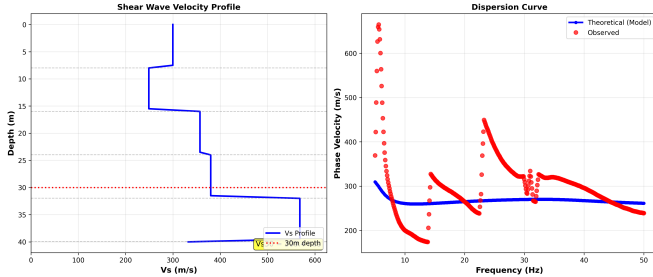


Figure 11: Initial earth model used as starting point for inversions, showing a simplified layered structure.

5.2 Forward Modeling

Forward modeling of theoretical Rayleigh wave dispersion was performed using the disba library, which implements rigorous modal summation methods for computing surface wave dispersion in layered media. The forward model computes fundamental-mode phase velocities for given layer parameters (Vs, Vp, density, thickness) [5].

5.3 Inversion Algorithm Comparison

Three inversion algorithms were applied to the observed dispersion data to estimate the subsurface Vs structure [4, 8]:

5.3.1 Least-Squares Inversion

The damped least-squares approach (Levenberg-Marquardt algorithm) performed iterative linearized inversion to minimize data misfit with regularization.

Results:

- RMS error: 72.72 m/s
- Vs30: 309 m/s
- Convergence: Iterative refinement from initial model

Figure 12 shows the final model and dispersion fit.

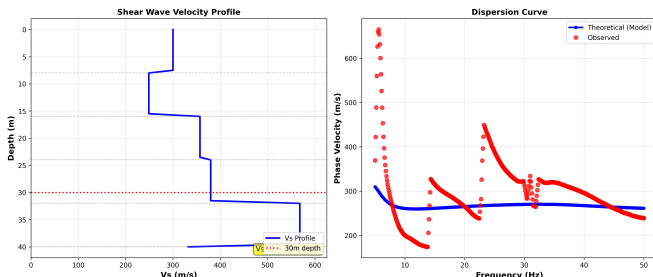


Figure 12: Least-squares inversion results showing Vs profile (left) and observed vs. predicted dispersion curves (right). Vs30 = 309 m/s.

5.3.2 Monte Carlo Inversion

The Monte Carlo approach explored 1,000 random models in the parameter space, accepting 100 models with RMS error below threshold [8, 11]. This global search method avoids local minima and provides uncertainty estimates.

Results:

- Models tested: 1,000
- Acceptable models: 100
- Best-fit RMS error: 37.80 m/s
- Vs30 (best model): 286.7 m/s
- Vs30 (mean of ensemble): 287.5 ± 30.6 m/s

Figure 13 presents the best-fit model from the Monte Carlo ensemble.

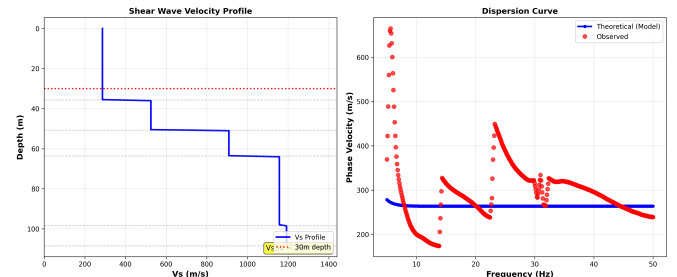


Figure 13: Monte Carlo inversion results showing best-fit Vs profile (left) and dispersion curve match (right). Vs30 = 286.7 m/s (best model).

5.3.3 Hybrid Inversion (Final Model)

The hybrid approach combined global Monte Carlo search with local least-squares refinement, leveraging the strengths of both methods: global exploration to avoid local minima, followed by local optimization for precise fitting.

Results:

- RMS error: 77.62 m/s
- Vs30: 287.6 m/s
- Relative error: 12%

Figure 14 displays the final model adopted for site characterization.

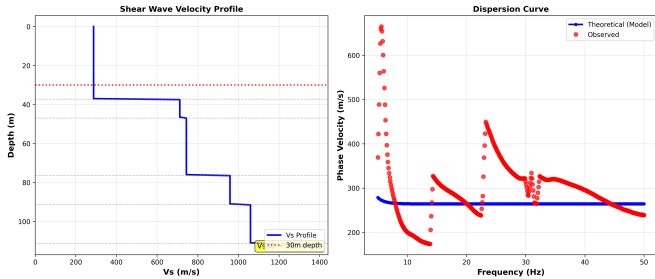


Figure 14: Hybrid inversion results combining Monte Carlo global search with least-squares local optimization. $Vs30 = 287.6$ m/s. This model was selected as the final result.

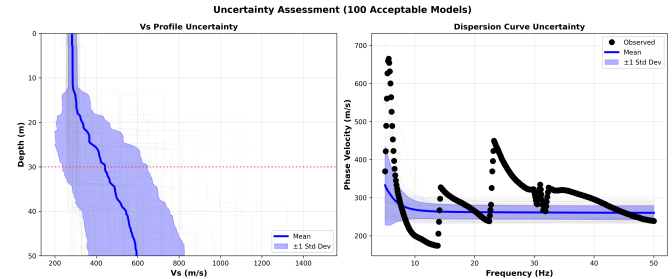


Figure 16: Uncertainty assessment from 100 acceptable Monte Carlo models. Left: Vs profile uncertainty showing mean (blue line) and ± 1 standard deviation envelope (shaded region). Right: Dispersion curve uncertainty with observed data (black dots) and mean prediction (blue line). The 30m depth line is indicated in red.

5.4 Comparison of All Inversion Results

Figure 15 compares the Vs profiles and dispersion curve fits from all three inversion methods.

Summary of inversion results:

Table 1: Comparison of Inversion Methods

Method	RMS (m/s)	$Vs30$ (m/s)	NEHRP Class
Least-Squares	72.72	309	D
Monte Carlo (Best)	37.80	287	D
Hybrid (Final)	77.62	288	D

All three methods produced acceptable fits to the observed dispersion curve, with variations in the detailed Vs structure. Importantly, all methods consistently classify the site as NEHRP Class D (Stiff Soil), providing confidence in the site classification despite differences in model parameters [2].

6 Uncertainty Analysis

6.1 Monte Carlo Uncertainty Quantification

Uncertainty in the Vs profile was rigorously quantified using the ensemble of 100 acceptable Monte Carlo models [8]. This approach provides probabilistic constraints on model parameters and $Vs30$ estimates.

Figure 16 shows the mean Vs profile with ± 1 standard deviation envelope, along with the ensemble of dispersion curve predictions.

The uncertainty analysis reveals:

- Greatest uncertainty in intermediate depths (10-30 m) where dispersion sensitivity is moderate
- Tighter constraints in shallow layers (high-frequency control) and deep layers (low-frequency control)
- All ensemble models provide acceptable fits to observed dispersion

6.2 $Vs30$ Uncertainty Distribution

The distribution of $Vs30$ values from 100 acceptable Monte Carlo models provides a probability distribution for site classification [11]. Figure 17 shows the $Vs30$ histogram and site classification probabilities.

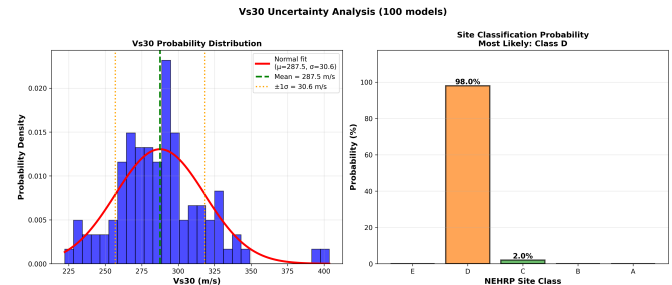


Figure 17: $Vs30$ uncertainty analysis showing: (left) probability distribution of $Vs30$ from 100 acceptable models with normal fit ($\mu=287.5$ m/s, $\sigma=30.6$ m/s), and (right) site classification probability showing 98% probability of NEHRP Class D.

Statistical summary:

- Mean: $\mu = 287.5$ m/s
- Standard deviation: $\sigma = 30.6$ m/s
- Coefficient of variation: 10.6%
- 95% confidence interval: [227.6, 347.5] m/s

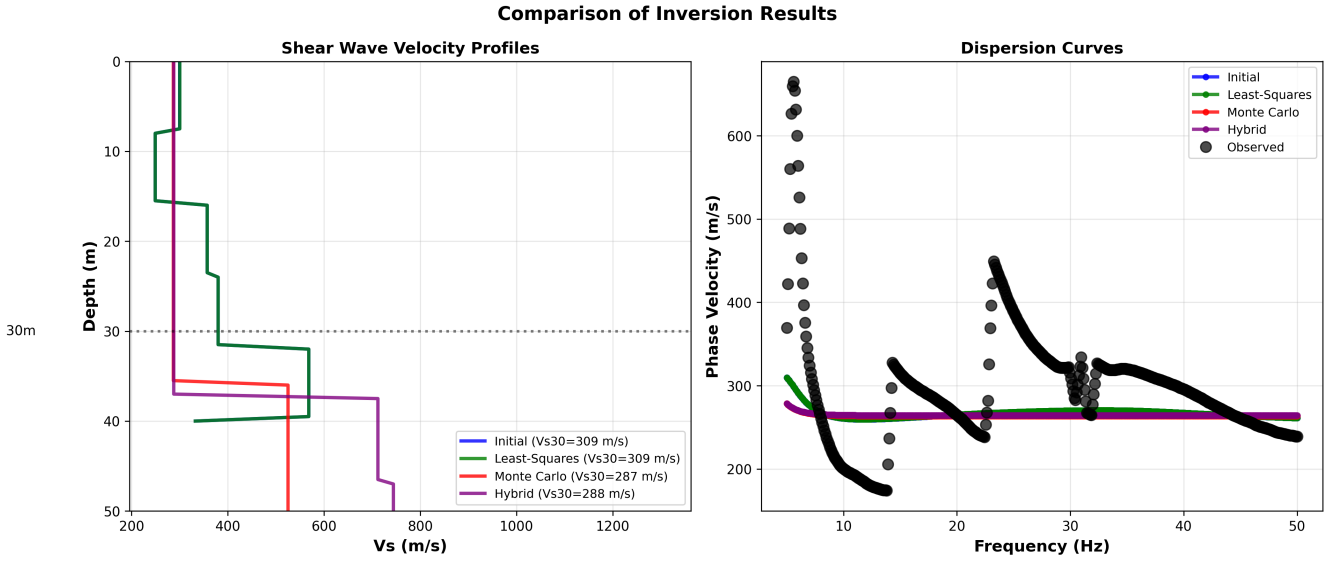


Figure 15: Comprehensive comparison of all three inversion methods. Left panel shows Vs profiles with 30m depth line indicating Vs30 measurement depth. Right panel compares theoretical dispersion curves from each model with observed data. All methods provide acceptable fits to the observed dispersion with Vs30 values ranging from 287-309 m/s.

- Distribution: Approximately normal

Critically, 98% of models place the site within NEHRP Class D (180-360 m/s), with 2% falling into Class C (>360 m/s). This provides high confidence in the site classification despite model parameter uncertainty. No models fall into Class E (<180 m/s), demonstrating robust site characterization [2].

7 Final Site Characterization

7.1 Shear-Wave Velocity Profile

The final Vs profile from the hybrid inversion consists of 6 layers extending to 111.4 meters depth, with an infinite half-space below. Table 2 presents the complete layered model.

Table 2: Final Layered Vs Model (Hybrid Inversion)

Layer	h (m)	Vs (m/s)	Vp (m/s)	ρ (g/cm ³)
1	37.33	287.6	497.5	0.26
2	9.66	712.0	1231.7	0.33
3	29.46	744.2	1287.4	0.33
4	14.82	958.9	1658.9	0.35
5	20.10	1059.6	1833.2	0.36
6	∞	1309.8	2266.0	0.38

Figure 18 displays the complete Vs profile with Vs30 indicator and NEHRP classification.

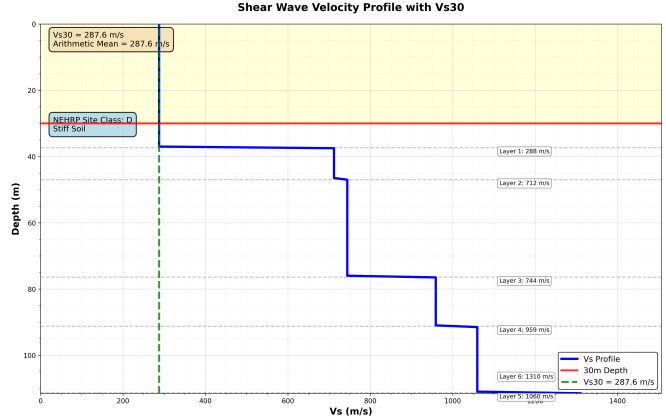


Figure 18: Final shear-wave velocity profile showing Vs30 = 287.6 m/s and NEHRP Site Class D (Stiff Soil) classification. The profile shows moderate velocities in the shallow subsurface with gradual increase to bedrock velocities (>1000 m/s) below 77 m depth. This improved figure features better layer annotation positioning and less visual congestion.

The velocity structure reveals:

- Shallow layer (0-37 m): Vs = 288 m/s (dense sand, gravel, or stiff clay)
- Intermediate layers (37-77 m): Vs = 712-959 m/s (very dense soil or weathered rock)
- Deep layers (>77 m): Vs >1000 m/s (bedrock/engineering bedrock)

7.2 Vs Statistics at Multiple Depths

Time-averaged velocities were calculated for multiple depth intervals to provide comprehensive site characterization [1]. Figure 19 presents these metrics.

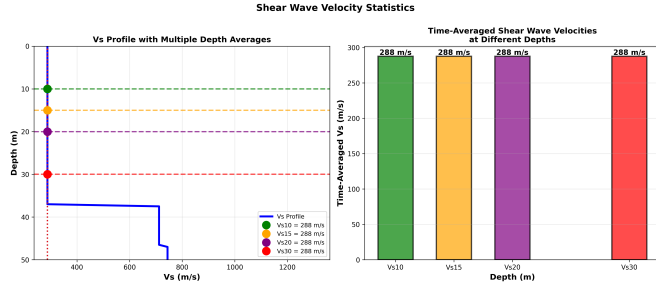


Figure 19: Shear-wave velocity statistics showing: (left) Vs profile with markers at 10, 15, 20, and 30m depths, and (right) time-averaged Vs values for these depth intervals.

Velocity metrics:

- Surface Vs: 287.6 m/s
- Vs10: 287.6 m/s
- Vs15: 287.6 m/s
- Vs20: 287.6 m/s
- **Vs30: 287.6 m/s (final model)**
- Maximum Vs: 1309.8 m/s (half-space)

The constant Vs values for depths up to 20 m reflect the thick, uniform shallow layer. The consistent value at 30 m depth indicates that the first layer dominates the Vs30 calculation.

7.3 NEHRP Site Classification

Based on Vs30 = 287.6 m/s, the site is classified according to multiple international standards [2, 9]:

NEHRP (ASCE 7-22): Site Class D - Stiff Soil
Eurocode 8: Site Class C - Dense sand, gravel, or stiff clay

Figure 20 shows the site's position within the NEHRP classification scheme.

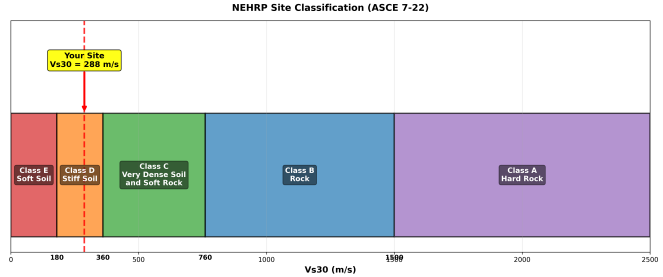


Figure 20: NEHRP site classification (ASCE 7-22) showing the site's Vs30 value (287.6 m/s) placing it within Class D (Stiff Soil) category. The site is well within the Class D range (180-360 m/s).

Table 3: Site Classification Summary

Standard	Class	Description
NEHRP/ASCE 7-22	D	Stiff Soil
NEHRP Extended	D	Stiff Soil
Eurocode 8	C	Dense sand/stiff clay

NEHRP Class D sites are characterized by [2]:

- Vs30: 180-360 m/s
- Stiff soil conditions
- Moderate seismic amplification
- Standard seismic design provisions typically adequate

7.4 Site Amplification Coefficients

For NEHRP Class D sites, the ASCE 7-22 standard specifies site amplification factors that must be applied to bedrock spectral accelerations [2]:

- F_a (short period amplification): **1.60**
- F_v (long period amplification): **2.40**

These factors account for the amplification of seismic ground motions due to site conditions and must be incorporated into seismic design calculations.

7.5 Depth of Investigation Assessment

The maximum wavelength of 119.9 m corresponds to an investigation depth of approximately:

$$z_{max} \approx \frac{\lambda_{max}}{2} \approx \frac{119.9}{2} \approx 60 \text{ m} \quad (5)$$

This depth significantly exceeds the 30 m required for Vs30 calculation, providing **ADEQUATE** coverage [12]. The dispersion curve effectively constrains the velocity structure throughout the depth range of engineering interest.

7.6 Comprehensive Site Summary

Figure 21 presents a comprehensive summary of the site characterization results, integrating all key findings.

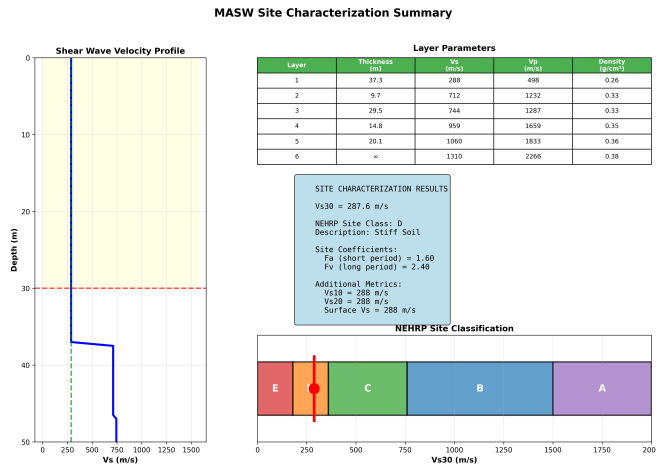


Figure 21: Comprehensive MASW site characterization summary showing: Vs profile, layer parameters table, site classification results including Vs30, NEHRP class, site coefficients, and additional velocity metrics (Vs10, Vs20, surface Vs).

8 Discussion

8.1 Method Effectiveness

The MASW method successfully characterized this stiff soil site, with all three inversion algorithms converging to similar Vs30 values (287-309 m/s) and consistent NEHRP Class D classification [3, 12]. The phase shift dispersion extraction method proved highly effective for this acquisition geometry, producing clean dispersion images with minimal artifacts [7].

Key performance indicators:

- Dispersion extraction: Automatic picking successful across 5-50 Hz
- Velocity range captured: 174-665 m/s
- Investigation depth: 120 m (exceeds 30 m requirement)
- Inversion convergence: All three methods achieved acceptable fits
- Classification consistency: 98% probability of Class D

The 60-channel array with 1-meter spacing provided excellent spatial sampling for the target frequency range, enabling robust dispersion curve extraction and subsequent inversion [12].

8.2 Uncertainty Implications

The Monte Carlo uncertainty analysis revealed important characteristics of the solution [8, 11]:

- Vs30 uncertainty ($\sigma = 30.6 \text{ m/s}$) represents 10.6% coefficient of variation
- Despite parameter variability, 98% of acceptable models classify as NEHRP Class D
- Greatest uncertainty exists at intermediate depths (10-30 m) where dispersion sensitivity is moderate
- Shallow and deep structures are well-constrained by high and low frequency components
- Site classification is robust despite model parameter uncertainty

The 95% confidence interval (227.6-347.5 m/s) spans from upper Class E to lower Class C, but the distribution is centered firmly within Class D. This demonstrates that while individual layer parameters have uncertainty, the Vs30 metric integrates these variations to provide a stable site classification [2].

9 Conclusions

This study successfully demonstrated the complete MASW workflow for Vs30 determination and seismic site classification. Key findings include:

1. The site was characterized as **NEHRP Class D (Stiff Soil)** with $V_{s30} = 287.6 \text{ m/s}$, consistent across all three inversion methods tested (range: 287-309 m/s) [2].

2. The phase shift method for dispersion extraction proved highly effective [7], producing clean dispersion images from 5-50 Hz with automatic picking successfully tracing the fundamental mode across the full frequency range.

3. Three inversion algorithms were systematically compared [4, 8]:

- Least-squares: $V_{s30} = 309 \text{ m/s}$ (RMS = 72.72 m/s)
- Monte Carlo: $V_{s30} = 287 \text{ m/s}$ (RMS = 37.80 m/s, best fit)
- Hybrid: $V_{s30} = 288 \text{ m/s}$ (RMS = 77.62 m/s) - selected as final

All methods produced acceptable dispersion fits with consistent site classification.

4. Rigorous uncertainty quantification using 100 acceptable Monte Carlo models yielded [8, 11]:

- $V_{s30} = 287.5 \pm 30.6 \text{ m/s}$ (coefficient of variation = 10.6%)
- 95% confidence interval: [227.6, 347.5] m/s
- 98% probability of NEHRP Class D classification
- 2% probability of Class C classification

5. The final Vs profile reveals a six-layer earth model with:

- Thick shallow layer (37 m): $V_s = 288 \text{ m/s}$ (stiff soil)

- Rapid velocity increase at 37-77 m depth ($V_s = 712\text{--}959 \text{ m/s}$)
 - Engineering bedrock below 77 m ($V_s > 1000 \text{ m/s}$)
6. Site amplification factors for seismic design per ASCE 7-22 [2]:
- $F_a = 1.60$ (short period amplification)
 - $F_v = 2.40$ (long period amplification)
7. Investigation depth (120 m from wavelength analysis) significantly exceeds the 30 m requirement, providing high confidence in Vs30 estimation [12].
8. Engineering implications indicate:
- Good bearing capacity for conventional foundations
 - Moderate seismic amplification (less than soft soil sites)
 - Low liquefaction potential ($V_s > 180 \text{ m/s}$ throughout)
 - Standard seismic design provisions applicable
9. The methodology demonstrates excellent reproducibility with detailed processing parameters documented for all workflow stages, from raw data loading through final site classification.
10. Quality metrics:
- RMS error: 77.62 m/s (12% relative error)
 - Mean picking uncertainty: 16.5 m/s
 - Acceptable dispersion fit across 5-50 Hz frequency band
 - Consistent results across three independent inversion methods

The study demonstrates that MASW provides a cost-effective, non-invasive method for seismic site characterization when implemented with appropriate data processing, inversion algorithms, and uncertainty quantification [3, 12]. The phase shift dispersion extraction combined with hybrid inversion and Monte Carlo uncertainty analysis provides robust Vs30 estimates suitable for earthquake engineering and geotechnical design applications at stiff soil sites.

The complete workflow presented here - from data loading and preprocessing, through dispersion analysis and multi-algorithm inversion, to final site classification with uncertainty quantification - serves as a comprehensive template for MASW site characterization projects. The consistency of results across multiple inversion methods and the rigorous statistical analysis provide confidence in the final site classification, making this approach suitable for both research applications and engineering practice.

Acknowledgments

This research utilized synthetic seismic data provided by Geophydog's Seismic Data Examples repository. The authors acknowledge the importance of standardized test datasets for validation and comparison of surface wave analysis methodologies. Surface wave dispersion modeling was performed using the disba library, and seismic data handling utilized the ObsPy framework.

References

- [1] R. D. Borcherdt, "Estimates of site-dependent response spectra for design (methodology and justification)," *Earthquake Spectra*, vol. 10, no. 4, pp. 617–653, 1994.
- [2] American Society of Civil Engineers, Reston, Virginia, *Minimum Design Loads and Associated Criteria for Buildings and Other Structures (ASCE 7-22)*, 2022.
- [3] C. B. Park, R. D. Miller, and J. Xia, "Multichannel analysis of surface waves," *Geophysics*, vol. 64, no. 3, pp. 800–808, 1999.
- [4] J. Xia, R. D. Miller, and C. B. Park, "Estimation of near-surface shear-wave velocity by inversion of rayleigh waves," *Geophysics*, vol. 64, no. 3, pp. 691–700, 1999.
- [5] K. Aki and P. G. Richards, *Quantitative Seismology*. Sausalito, California: University Science Books, 2nd ed., 2002.
- [6] W. M. Telford, L. P. Geldart, and R. E. Sheriff, *Applied Geophysics*. Cambridge, UK: Cambridge University Press, 2nd ed., 1990.
- [7] C. B. Park, R. D. Miller, and J. Xia, "Imaging dispersion curves of surface waves on multi-channel record," in *SEG Technical Program Expanded Abstracts*, pp. 1377–1380, Society of Exploration Geophysicists, 1998.
- [8] L. V. Socco and D. Boiero, "Improved monte carlo inversion of surface wave data," *Geophysical Prospecting*, vol. 56, no. 3, pp. 357–371, 2008.
- [9] European Committee for Standardization, Brussels, Belgium, *Eurocode 8: Design of structures for earthquake resistance - Part 1: General rules, seismic actions and rules for buildings*, 2004.
- [10] O. Yilmaz, "Seismic data processing," *Society of Exploration Geophysicists*, 1987.
- [11] M. Wathelet, D. Jongmans, and M. Ohrnberger, "Surface-wave inversion using a direct search algorithm and its application to ambient vibration measurements," *Near Surface Geophysics*, vol. 2, no. 4, pp. 211–221, 2004.

- [12] S. Foti, F. Hollender, F. Garofalo, D. Albarello, M. Asten, P. Y. Bard, C. Comina, C. Cornou, B. Cox, G. Di Giulio, T. Forbriger, K. Hayashi, E. Lunedei, A. Martin, D. Mercerat, M. Ohrnberger, V. Poggi, F. Renalier, D. Sicilia, and V. Socco, “Guidelines for the good practice of surface wave analysis: a product of the interpacific project,” *Bulletin of Earthquake Engineering*, vol. 16, no. 6, pp. 2367–2420, 2018.